IMMUNOLOGY

From hit to vial: Precision discovery and development of an imidazopyrimidine TLR7/8 agonist adjuvant formulation

Dheeraj Soni[1,2]†, Francesco Borriello[1,2]‡, David A. Scott[2,3], Frederic Feru[2,3], Maria DeLeon[1,2], Spencer E. Brightman[1], Wing Ki Cheng[1,2], Gandolina Melhem[1,2], Jennifer A. Smith[2], Juan C. Ramirez[1,2], Soumik Barman[1,2], Michael Cameron[4], Aisling Kelly[1], Kristina Walker[1], Etsuro Nanishi[1,2], Simon Daniel van Haren[1,2], Tony Phan[5], Yizhi Qi[5], Robert Kinsey[5], Michal M. Raczy[6], Al Ozonoff[1,2,7], Matthew A. Pettengill[1,2]§, Jeffery A. Hubbell[6], Christopher B. Fox[5,8], David J. Dowling[1,2]*¶, Ofer Levy[1,2,7]*¶

Vaccination can help prevent infection and can also be used to treat cancer, allergy, and potentially even drug overdose. Adjuvants enhance vaccine responses, but currently, the path to their advancement and development is incremental. We used a phenotypic small-molecule screen using THP-1 cells to identify nuclear factor-κB (NF-κB)–activating molecules followed by counterscreening lead target libraries with a quantitative tumor necrosis factor immunoassay using primary human peripheral blood mononuclear cells. Screening on primary cells identified an imidazopyrimidine, dubbed PVP-037. Moreover, while PVP-037 did not overtly activate THP-1 cells, it demonstrated broad innate immune activation, including NF-κB and cytokine induction from primary human leukocytes in vitro as well as enhancement of influenza and SARS-CoV-2 antigen-specific humoral responses in mice. Several de novo synthesis structural enhancements iteratively improved PVP-037's in vitro efficacy, potency, species-specific activity, and in vivo adjuvanticity. Overall, we identified imidazopyrimidine Toll-like receptor-7/8 adjuvants that act in synergy with oil-in-water emulsion to enhance immune responses.

INTRODUCTION

Vaccination remains one of the most cost-effective health interventions available, significantly reducing morbidity, and preventing 2 million to 3 million deaths every year from vaccine-preventable infectious diseases such as diphtheria, tetanus, pertussis, measles, influenza, and COVID-19 (*1*). In addition, vaccine indications include prevention of cancer (e.g., human papillomavirus vaccine and hepatitis B vaccine) as well as discovery and development of vaccines for drug (e.g., opioid) overdose (*2*–*5*). Contemporary vaccine strategies generally target defined antigens, using a broad set of platforms, including purified recombinant proteins and genetic delivery (*6*). Although this approach has lowered reactogenicity of many clinically licensed formulations, vaccine efficacy may lag because of insufficient innate immune stimulation that can enhance magnitude, breadth, and durability of vaccine-induced immunity (*7*). Adjuvants can enhance vaccine responses by activating pattern-recognition receptors (PRRs) and/or by modulating antigen pharmacokinetics (*8*, *9*).

[1]Precision Vaccines Program, Department of Pediatrics, Boston Children's Hospital, Boston, MA, USA. [2]Harvard Medical School, Boston, MA, USA. [3]Dana-Farber Cancer Institute, Boston, MA, USA. [4]Department of Molecular Medicine, The Scripps Research Institute, Jupiter, FL, USA. [5]Access to Advanced Health Institute (AAHI), Seattle, WA, USA. [6]Pritzker School of Molecular Engineering, University of Chicago, Chicago, IL, USA. [7]Broad Institute of MIT & Harvard, Cambridge, MA, USA. [8]Department of Global Health, University of Washington, 3980 15th Ave NE, Seattle, WA 98195, USA.
*Corresponding author. Email: ofer.levy@childrens.harvard.edu (O.L.); david.dowling@childrens.harvard.edu (D.J.D.)
†Present address: Global Investigative Toxicology, Preclinical Safety, Sanofi, Cambridge, MA, USA.
‡Present address: Generate Biomedicines, Somerville, MA, USA.
§Present address: Department of Pathology, Anatomy, and Cell Biology, Thomas Jefferson University Hospital, Philadelphia, PA, USA.
¶These authors contributed equally to this work.

Many first-generation 20th-century vaccines, consisting of live attenuated or inactivated vaccines, expressed immune-stimulating components and therefore are "self-adjuvanted" (*10*). Multidisciplinary investigations of innate immunity and systems vaccinology have further informed discovery and development of novel adjuvants, which is now being accelerated by a need for use of an expanded group of adjuvanted vaccines against COVID-19 and future pandemics (*11*).

However, alum- and emulsion-based adjuvanted vaccines often require multiple doses for definite protection and primarily drive T helper 2 (T_H2)–based immunity. To overcome the former, adjuvant combinations of aluminum salts, oil-in-water (O/W) emulsions in combination with PRR agonists have been shown to enhance vaccine immune responses compared to aluminum salts, emulsions, or PRR agonists alone (*12*). AS04 was the first adjuvant system (AS) composed of aluminum salts and a PRR agonist, specifically the Toll-like receptor 4 (TLR4) agonist monophosphoryl lipid A (MPLA), to be included in licensed vaccines for human papillomavirus and hepatitis B vaccines (*12*). AS01, consisting of MPLA and the purified plant bark extract/saponin QS21, is the AS in the Mosquirix (RTS,S) malaria vaccine (*13*, *14*). Adjuvants directed toward the endosomal TLRs 7, 8, and 9 have demonstrated robust T_H1-polarizing activity, especially in immunologically distinct populations (*15*–*17*). Thus, combinations of emulsions and T_H1-polarizing PRR agonists represent a promising adjuvant strategy to enhance antigen-specific immunity. Adjuvants can substantially reduce the amount of antigen needed to induce sufficient immunity, which is key to increase global vaccine supplies, especially relevant during pandemics (*18*).

High-throughput screening (HTS) is a powerful approach for drug discovery. However, phenotypic adjuvant discovery HTS has

been largely limited to use of cell lines, which are convenient to culture and provide high consistency in readouts, but do not always accurately reflect the responses of primary leukocytes nor of the diverse human immune system (*19*–*21*). In this regard, using primary human leukocytes for HTS may improve and more accurately predict efficacy and toxicity of lead adjuvant candidates early in the drug discovery programs. However, several challenges have been identified in screening paradigms that leverage primary cells (*22*), contributing to the dearth of primary cell screening campaigns.

Here, we outline the discovery of an imidazopyrimidine (IMP), a TLR7/8 agonist (TLR7/8A) adjuvant, named PVP-037 (the 37th small molecule named within the Precision Vaccines Program adjuvant portfolio), via a phenotypic peripheral blood mononuclear cell (PBMC) HTS. In addition, we outline some unique innate immunological properties of the PVP-037 adjuvant, medicinal chemistry optimization, insights into the adjuvant's in vitro and in vivo mechanism of action, and demonstration of markedly enhanced T_H1-skewed immune responses toward influenza antigens in mice in a prime-boost immunization schedule. Furthermore, we optimized a stable O/W formulation incorporating PVP-037, which synergistically enhanced vaccine-specific antibody (Ab) titers compared to adjuvant alone. Overall, we outline the discovery and development of an IMP adjuvant from original HTS hit through creation of a stable vial of the candidate adjuvant formulation that may have utility in vaccines for indications requiring enhancement of T_H1-polarized immune responses.

RESULTS

Counterscreening using human primary PBMCs identifies potent tumor necrosis factor–inducing molecule

First, ~200,000 small molecules were screened via a THP1-Lucia based nuclear factor κB (NF-κB)–induced luminescence assay. Approximately 10,000 molecules were identified as hits, across ~20 enriched library plates (Fig. 1A and table S1). Next, we used a unique HTS approach by using primary human cells for screening of small molecules with immunomodulatory properties (Fig. 1A). Human blood was collected from three adult male donors, and PBMCs were harvested and cryopreserved, generating three unique PBMC biobanks (fig. S1A). Each participant biobank was generated over a ~6- to 8-month period, totaling ~1×10^9 cells per donor. Counterscreening of immunogenic molecules was performed using a ~10,000 small-molecules library (curated from the ~20 enriched library plates) via a no-wash 384-well quantitative tumor necrosis factor (TNF) immunoassay (table S2). Preliminary hits were based on TNF induction in at least two of the three donors screened. Using statistical hit calling measures, ~250 potential hits were identified, among which ~25 were confirmed hits as validated with enzyme-linked immunosorbent assay (ELISA)–based titration assays

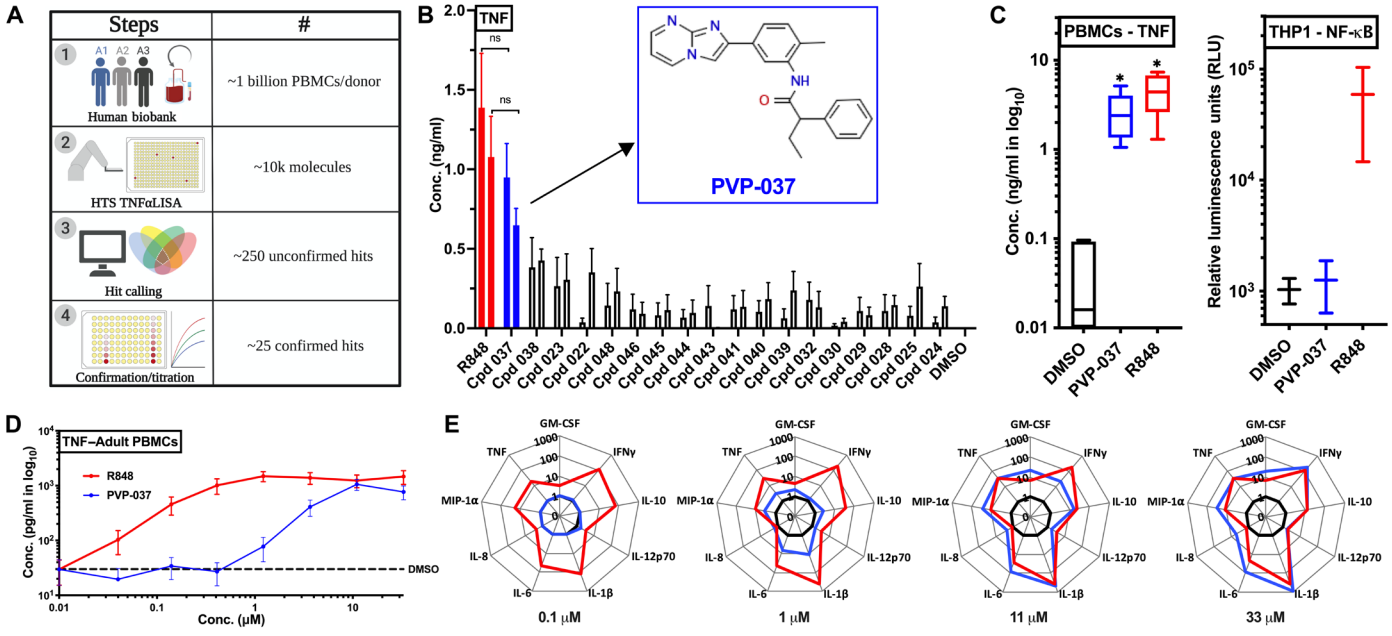

Fig. 1. High-throughput in vitro screening of primary human PBMCs identified PVP-037, an imidazopyrimidine small-molecule that induces cytokine production. (**A**) Schematic diagram depicting HTS of small-molecules with adjuvant effect using peripheral blood mononuclear cells (PBMCs) from adult human donors. A human bio-bank for PBMCs was created by drawing blood from donors over ~6 to 8 months. Downselecting from ~200,000 molecules via a HTS cell line screen, PBMC screening for immunomodulatory molecules was performed using a ~10,000 small-molecule library, via a no-wash 384-well quantitative TNF immunoassay from three adult healthy human donors. Preliminary hits were based on induced TNF production in at least two of the three donors screened. Using statistical analyses, ~250 potential hits were identified, among which ~25 established hits were confirmed with ELISA-based titration assays. (**B**) Titration of identified hits was performed using adult human PBMCs and TNF production over 18 hours of incubation. PVP-037 emerged as the lead molecule with activity similar to R848 at 33 and 11 μM, respectively. Chemical structure of PVP-037 is shown within the graph. $n = 5$ donors. (**C**) PVP-037 induced TNF in PBMCs as compared to R848. PVP-037 lacks NF-κB–inducing activity in cell lines (e.g., monocytic THP-1 cell line). $n = 5$ donors for PBMCs and two independent experiments for THP-1 screen. (**D**) Human adult PBMCs were stimulated with PVP-037 or R848 in an eight-point concentration titration manner for 18 hours and supernatant processed for TNF production or (**E**) 10 plex cytokines analysis. $n = 8$ donors.

(fig. S1B). Resiquimoid (R848), a synthetic small-molecule imidazoquinoline TLR7/8A, served as a benchmark for these screens. Among the ~10,000 molecules tested, an IMP, which we named Precision Vaccines Program-037 (PVP-037), emerged as the most promising hit, based on its ability to induce TNF production in human PBMCs, with comparable in vitro efficacy to R848 (Fig. 1B). Further, we re-evaluated activity of PVP-037 in primary cells (i.e., human PBMCs) versus THP-1 cells (human monocytic cell line). PVP-037 maintained significant immunomodulatory activity in human PBMCs, comparable to R848. However, it lacked any activity in the human THP-1 monocytic cell line, highlighting the distinct nature of this IMP scaffold and lack of prior identification (Fig. 1C). To characterize its potency, we titrated PVP-037 in an eight-point curve for stimulating human PBMCs and observed concentration-dependent activity for inducing cytokine production. At concentrations ≥11 μM, PVP-037 induced TNF in human PBMCs to a similar extent as R848 (Fig. 1D). PVP-037 induced cytokine and chemokine production from primary human PBMCs at concentrations ≥1 μM, including TNF, granulocyte-macrophage colony-stimulating factor (GM-CSF), interferon-γ (IFNγ), interleukin-10 (IL-10), IL-12p70, IL-1β, IL-6, and CCL3 (MIP1α). At ≥11 μM, PVP-037 induced T_H1-polarizing cytokines comparable to matching concentrations of R848, including TNF, IFNγ, IL-1β (Fig. 1E).

PVP-037 SAR identifies highly potent analogs in vitro that are effective adjuvants in vivo

We next pursued structure activity relationship (SAR) studies to optimize PVP-037 for downstream formulation and applicability as an adjuvant via (i) purchase of commercially available analogs and (ii) de novo synthesis (core substituent analogs) (Fig. 2A). Commercially available analogs were identified to explore the amide SAR of PVP-037. Of this set, the 2-trifluoromethyl benzamide (referred to as Cpd 37.37) induced the highest TNF production in human PBMCs (Fig. 2A, left). Next, we prepared analogs of Cpd 37.37 with modifications to the IMP core and central phenyl ring (Fig. 2A, right). We found that the introduction of a methyl group to the IMP core (Cpd 2-144-3) enhanced TNF-inducing activity. We also replaced the IMP core with alternative bicyclic ring systems (fig. S2) but observed reduced activity in all cases. For the full set of analogs, we observed a similar rank order of activity in human PBMCs and murine splenocytes (fig. S3). Cpd 2-144-3, subsequently referred to as PVP-037.1, activated both human PBMCs (Fig. 2B) and mouse splenocytes (Fig. 2C). PVP-037.1 also demonstrated enhanced induction of TNF in porcine PBMCs in vitro (fig. S4).

PVP-037 demonstrated adjuvanticity in mice immunized with recombinant hemagglutinin protein (rHA) in vivo (Fig. 2D). Mice immunized with rHA admixed PVP-037 demonstrated higher Ab titers compared to mice immunized with rHA alone and equivalent or enhanced titers as compared to mice immunized with rHA and Alum, the most commonly used vaccine adjuvant. Notably, the highest immunoglobulin G (IgG) responses were observed in mice receiving rHA + PVP-037.1, demonstrating correlation of in vitro and in vivo activities (Fig. 2D). Further supporting its potential utility as an adjuvant, PVP-037.1 also demonstrated enhanced PK/ADME profile (fig. S5) as well as robust adjuvanticity via subcutaneous immunization (fig. S6). Conversely, an inactive analog, Cpd 02-184-2, did not enhance anti-rHA Ab titers (Fig. 2D), which correlated with lack of in vitro activity (fig. S2).

Amine derivative of PVP-037.1 has improved solubility, enhanced in vitro potency, and in vivo adjuvanticity

To enhance downstream formulation approaches, we installed a primary amine group on the phenyl ring of PVP-037.1, generating PVP-037.2 (Fig. 3A). This compound demonstrated improved solubility, facilitating subsequent formulation studies. Pleasingly, upon evaluation via human PBMC in vitro assays, we observed that PVP-037.2 had greater TNF-inducing efficacy, and notably, PVP-037.2 showed lower median effective concentration compared to PVP-037.1 and R848 (Fig. 3B). In addition, the amine addition also improved the in vivo profile of the analog. Mouse pharmacokinetic evaluation of drug serum concentrations at 8 hours after administration demonstrated that relative to PVP-037.1, PVP-037.2 had enhanced clearance from blood plasma and negligible hemolytic activity (Fig. 3C).

Furthermore, we evaluated adjuvant effect of PVP-037 analogs in vivo. We immunized adult (~6- to 8-week-old) C57BL/6J mice IM using a prime-only schedule using trivalent rHA influenza vaccine Flublok as a clinically relevant model antigen that is devoid of adjuvant, alone or formulated with PVP-037.1 or PVP-037.2 (100 nmol per mouse), and Ab titers for rHA-specific total IgG were measured by ELISA 28 days after immunization (Fig. 3D). We also investigated the titers of the IgG subclasses IgG1 and IgG2c, respectively associated with type 2 and type 1 (IFNγ-driven) immunity (*23*, *24*). As expected, both PVP-037.1 and PVP-037.2 increased anti-rHA IgG titers in adult mice. In line with our in vitro observations, only PVP-037.2 significantly enhanced antigen-specific IgG1 and IgG2c production after a single dose immunization (Fig. 3D).

To characterize the adjuvanticity of PVP-037.2, we expanded our evaluation to a second antigen. C57BL/6J adult mice were injected IM prime (day 0) with saline, wild-type (WT) SARS-CoV-2 spike protein alone, spike admixed with PVP-037.2 (100 nmol per mouse). Ab titers for WT spike-specific total IgG, IgG1 or IgG2c were measured by ELISA 28 days after immunization. Again, PVP-037.2 via a single dose immunization, drove enhancement of total IgG, IgG1, and IgG2c. Young mice (6 to 8 weeks old) vaccinated with PVP-037.2 maintained normal weight gains (fig. S7). In addition, PVP-037.2 demonstrated robust adjuvanticity across mouse strains (fig. S8). Via a prime-boost (day 28) schedule, PVP-037.2 hACE2-RBD (WT) inhibition was determined 42 days after immunization (Fig. 3E). Overall, these results support robust Ab enhancement via IMPs based adjuvants for multiple routes and antigens. Additionally, PVP-037.2 induced concentration-dependent production of TNF and IL-1β in human elder PBMCs in vitro, and showed adjuvanticity in aged mice when admixed with rHA (FluBlok vaccine; fig. S9).

PVP-037.2 demonstrates a TLR7/8-dependent immunomodulatory profile

As with our THP-1 data, initial in vitro evaluation of IMP family analogs via human embryonic kidney (HEK) 293 cells expressing human a TLR7 NFκB-SEAP reporter from Novus Biologicals (Littleton, CO) and InvivoGen (San Diego, CA) respectively, demonstrated undetectable activity. However, because (i) we have previously demonstrated that endosomal receptors are disproportionately the target for small-molecule agonists (*17*), and (ii) published reports have outlined difficulties reproducing TLR7/8 specificity using HEK293-hTLR7 cells (*25*), we investigated the activity of PVP-037.2 in PBMC

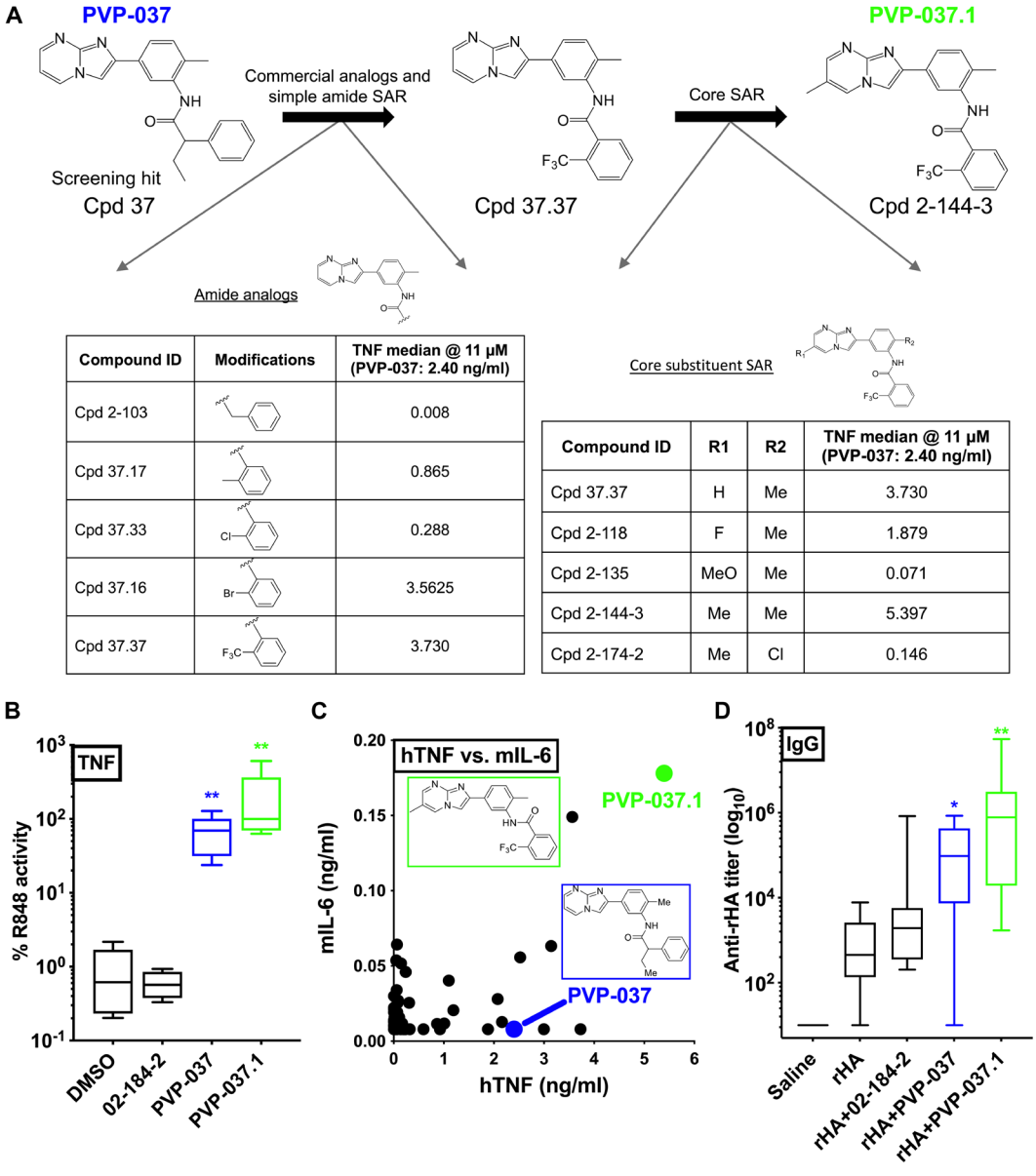

Compound ID	Modifications	TNF median @ 11 μM (PVP-037: 2.40 ng/ml)
Cpd 2-103		0.008
Cpd 37.17		0.865
Cpd 37.33		0.288
Cpd 37.16		3.5625
Cpd 37.37		3.730

Compound ID	R1	R2	TNF median @ 11 μM (PVP-037: 2.40 ng/ml)
Cpd 37.37	H	Me	3.730
Cpd 2-118	F	Me	1.879
Cpd 2-135	MeO	Me	0.071
Cpd 2-144-3	Me	Me	5.397
Cpd 2-174-2	Me	Cl	0.146

Fig. 2. Iterative PVP-037–based SAR identified highly potent analogs in vitro that were effective adjuvants in vivo. (**A**) Commercially available analogs of PVP-037 were purchased. The activity of these analogs at 11 μM were compared against PVP-037 in human PMBCs, of which 37.37 was identified to have enhanced activity. Further analogs of Cpd 37.37 were then prepared to explore the SAR of the IMP series. The tables depict the amount of TNF produced by representative analogs in a human PBMC stimulation assay with an 18-hour incubation period. Cpd 2-144-3 referred to as PVP-037.1 was identified as the most potent molecule. (**B**) TNF production after stimulation of human adult PBMCs with PVP-037 and two analogs for 18 hours at 33 μM, presented as % of intradonor R848 response. Results are presented as box-and-whisker plots ($n = 5$). $^{**}P < 0.01$ of PVP molecules versus DMSO by repeated measure one-way ANOVA of log-transformed data. Results represent median ± SEM. (**C**) Human adult PBMCs and murine splenocytes were stimulated with PVP-037 and its analogs for 18 hours at 33 μM. Each dot represents the median production of human TNF ($n = 5$) and murine IL-6 ($n = 6$) for each compound. Chemical structures of PVP-037 and PVP-037.1 are shown within the graph. (**D**) C57BL/6J adult mice (6 to 8 weeks old) were injected intramuscular (IM) prime (day 0)/boost (day 28) with saline, rHA alone, or rHA admixed with the indicated molecules. Titers for rHA-specific total IgG were measured by ELISA 42 days after immunization. Results are presented as box-and-whisker plots of 9 to 10 mice per group (saline, $n = 4$, alum, $n = 2$). $^{*}P < 0.05$, $^{**}P < 0.01$ of rHA + PVP molecules versus rHA by repeated measure one-way ANOVA of $\log_{10}$-transformed data. Results represent median ± SEM.

after the treatment with the short single-stranded oligodeoxynucleotides (ODN) 2088, a known TLR7/8/9 antagonist. Here, we observed near total loss of activity of PVP-037.2 (Fig. 4A). Furthermore, in human PBMCs, ODN 20958 (TLR7 specific antagonist) completely blocked PVP-037.2-induced TNF production, mirroring the response of CL264, a highly selective TLR7A. To confirm this observation, we also unraveled the mechanistic pathways induced by PVP-037 analogs using bone marrow–derived macrophages (BMDM) from both WT and *Tlr7*$^{-/-}$ mice. Here, both PVP-037.1- and PVP-037.2-induced TNF production, was significantly reduced in BMDMs from *Tlr7*$^{-/-}$ mice as compared to WT. Similar results were obtained with CL264 and R848, both

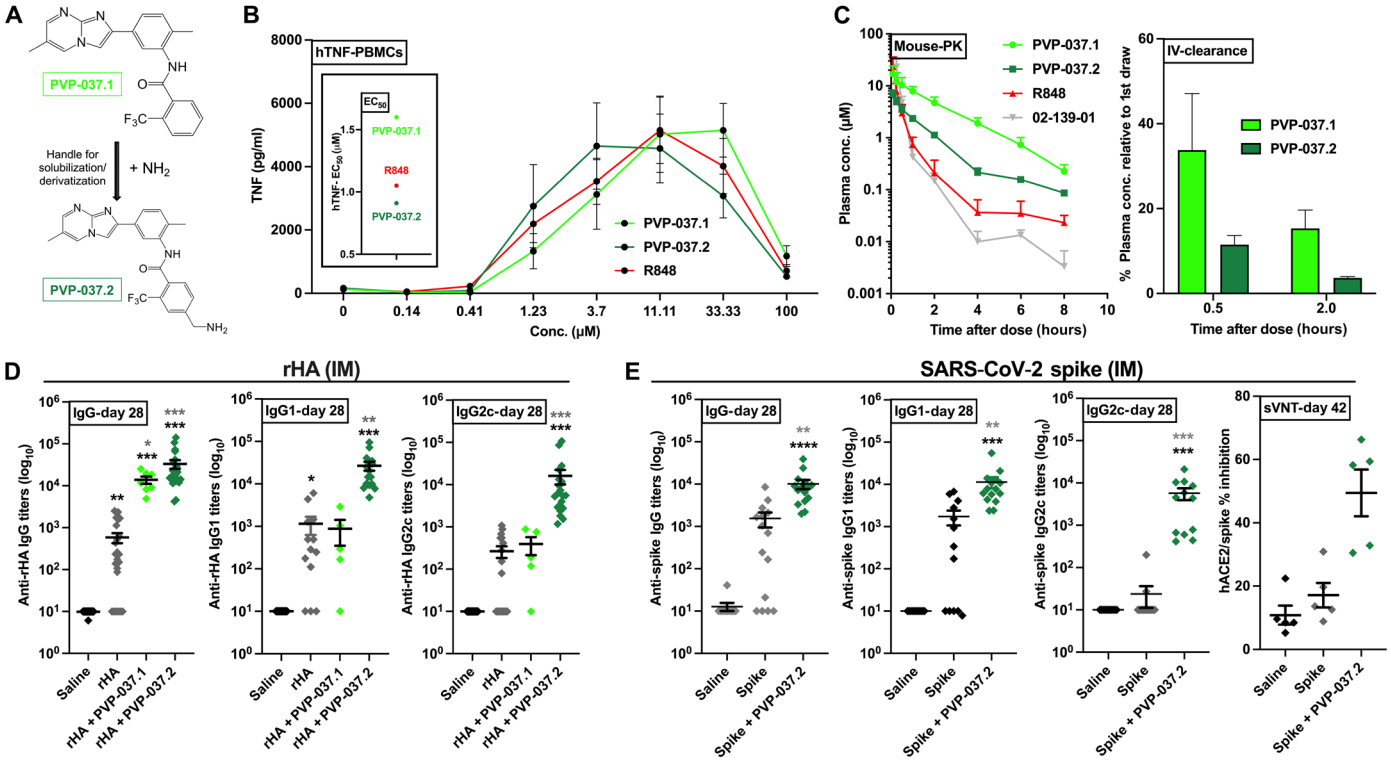

Fig. 3. Amine derivative PVP-037.2 has enhanced potency in vitro and adjuvanticity in vivo. (**A**) An amine tag was added to PVP-037.1. (**B**) PVP-037.2 was identified as a potent analog. After stimulation of human adult PBMCs for 18 hours. $n = 8$ donors. (**C**) To evaluate PK (drug serum levels), C57BL/6J adult mice weighing 20 to 30 g received a single formulation administration intravenously of 20 μl per mouse, at 3 mg/kg. Blood was collected (tail vein) from the same mouse before (0 min) and 0.1, 0.25, 0.5, 2, 4, 6, and 8 hours after administration. Left indicates plasma concentration over time. Right indicates % plasma concentration relative to baseline. (**D**) C57BL/6J mice were injected IM prime (day 0) with saline, rHA, and rHA admixed with the indicated adjuvants. Graphs represents antibody titers at day 28. (**E**) C57BL/6J adult mice were injected IM prime (day 0) with saline, WT spike protein, and spike admixed with PVP-037.2 (100 nmoles per mouse). Graphs represent antibody titers at day 28 (effect of single-dose immunization). hACE2-RBD (WT) inhibition rate was determined at day 42. In vitro results are presented as line graph ($n = 5$). $^*P < 0.05$, $^{**}P < 0.01$, $^{***}P < 0.001$, $^{****}P < 0.0001$ of small molecules versus DMSO by repeated measure one-way ANOVA of log-transformed data. In vivo results are 5 to 25 mice per group (except, sVNT $n = 5$). $^*P < 0.05$, $^{**}P < 0.01$ of rHA + PVP molecules versus rHA by repeated measure one-way ANOVA of $\log_{10}$-transformed data.

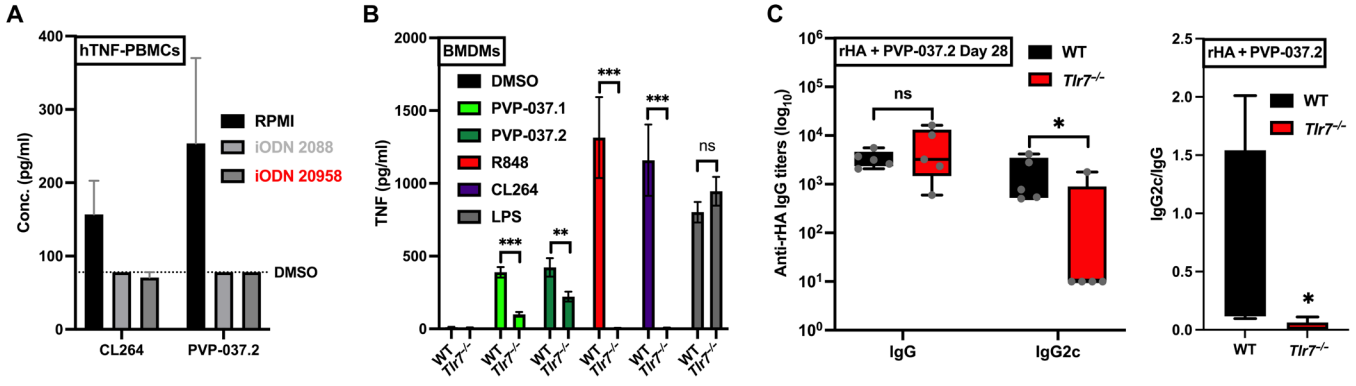

Fig. 4. PVP-037.2 demonstrates TLR7-dependent enhancement of T_H1-polarizing adjuvanticity. (**A**) PBMCs from adult human donors were incubated with inhibitory (i)ODNs (TLR7/8/9 antagonists consisting of short single-stranded oligodeoxynucleotides) and either ODN 2088 (TLR7/8/9 antagonist) or ODN 20958 (TLR7 antagonist) for 1 hour. After inhibition with iODNs, cells were stimulated with CL264 (TLR7A) or PVP.037.2, and supernatants were harvested after 20 to 24 hours. TNF production was assayed in the supernatants via ELISA ($n = 6$ donors). (**B**) Bone marrow was isolated from WT or *Tlr7*$^{-/-}$ mice to generate BMDMs, which were stimulated with 33 μM CL264 (TLR7A) or R848 (TLR7/8A), LPS (100 ng/ml) (TLR4A), 100 μM PVP-037.1, or PVP-037.2. The supernatants were collected after 20 to 24 hours, and TNF production was measured via ELISA ($n = 5$ samples). (**C**) WT or *Tlr7*$^{-/-}$ mice (6 to 8 weeks old) were injected IM prime with saline, rHA alone, and rHA admixed with the 100 nmol of PVP-037.2. Ab titers for rHA-specific total IgG or IgG2c were measured by ELISA 28 days after immunization ($n = 5$ samples).

known TLR7A. In contrast, responses to LPS were unaffected in *Tlr7*$^{-/-}$ BMDMs (Fig. 4B). On the basis of these in vitro observations, we evaluated the in vivo adjuvanticity of a single dose of PVP-037.2 toward rHA using WT and *Tlr7*$^{-/-}$ adult mice. Ab titers for rHA-specific total IgG or IgG2c were measured at 28 days after immunization. A significant reduction in IgG2c class switched Ab response was observed in the *Tlr7*$^{-/-}$ mice (Fig. 4C), strongly suggesting that the type 1 immunomodulatory profile of PVP-037.2 is mediated by TLR7. To further investigate the mechanism of action of PVP-037.2, we stimulated multiple HEK293 cell lines and assessed NF-κB activation in cells expressing hTLR2, hTLR3, hTLR4, hTLR5, hTLR8, or hTLR9. Notably, PVP-037.2 demonstrated activity in HEK-hTLR8 cells, while it did not induce any detectable activity in HEK-hTLR2, HEK-hTLR3, HEK-hTLR4, HEK-hTLR5, and HEK-hTLR9 cells (fig. S10).

Formulation of PVP-037.2 with squalene enhanced its adjuvanticity

Since the introduction of MF59, which enhances both humoral and cell mediated responses, O/W emulsions have been routinely used in many seasonal and pandemic influenza vaccines for adults (*26*–*28*). Combination ASs can be a powerful approach to enhance antigen-specific immunity (*29*). As with any pharmacologic agents, adjuvant combinations can demonstrate additivity, antagonism, or synergy (*30*). Several ASs, such as those developed by GlaxoSmithKline (GSK), are combination systems such as AS01 (MPLA + QS21 in liposomes), AS02 (MPLA + QS21 in O/W emulsion), AS03 (squalene + alpha-tocopherol in O/W emulsion), and AS04 (MPL + alum). Next, we undertook a formulation strategy for PVP-037.2, with various emulsion compositions (PVP-037.2/SE) (Fig. 5A).

An initial effort to develop a squalene emulsion with 1-palmitoyl-2-oleoyl-sn-glycero-3-phosphocholine as the emulsifier resulted in favorable emulsion droplet size (92 ± 1.2 nm) and a fairly narrow size distribution [polydispersity index (PDI) 0.117 ± 0.008]. However, only ~10% of the loaded PVP-037.2 was incorporated in the emulsion droplets. To increase compound incorporation, half of the squalene content was substituted with grapeseed oil in an effort to create more physical void spaces for compound entrapment in the oil core, as plant-derived oils have a more diverse profile of fatty acids with different saturation states that give rise to nonuniform molecular packing (*31*). In addition, a small amount of methanol and chloroform mixture (1:2, v/v) was used to solubilize the compound during the formulation process, which was subsequently removed by evaporation. These changes increased the initial PVP-037.2 incorporation to 56%. However, the incorporated PVP-037.2 gradually precipitated from the formulation over time, with the percent of compound retention down to 11% 10 days after formulation.

To promote complexation of PVP-037.2 with the emulsion, a modified formulation using a slightly acidic pH and an anionic emulsifier was devised. The formulation was prepared by adding a stock solution of PVP-037.2 in ethanol and 0.2% v/v HCl to emulsion components that included 1,2- myristoyl-sn-glycero-3-phosphocholine (DMPC), 1,2-dipalmitoyl-sn-glycero-3-[phospho-rac-(1-glycerol)] (DPPG), poloxamer 188, squalene, glycerol, and ammonium phosphate buffer, followed by water bath sonication at elevated temperature to generate a nanoemulsion. Following sonication, the ethanol was removed by dialysis and the final emulsion was filtered and filled into glass vials. As a control, blank emulsions were manufactured in a similar manner without PVP-037.2 (Fig. 5B). PVP-037.2 stable O/W emulsion (SE) demonstrated ≥90% adjuvant incorporation, acceptable particle size (~160 nm) and narrow particle size distribution (PDI < 0.17) (Fig. 5C). Adjuvant incorporation within PVP-037.2/SE and particle size were stable for at least 2 months, indicating potential for long term formulation stability (Fig. 5D) (*32*).

O/W emulsions (*26*–*28*) and TLR7/8As (*33*–*35*) induce distinct, though partially overlapping, innate immune activation (*36*), inducing production of innate type 1 interferon, pro-inflammatory cytokines and chemokines important to initiation of adaptive immune responses. Next, via use of murine RAW264.7 macrophage cells (expressing secreted embryonic alkaline phosphatase (SEAP) reporter construct, inducible by NF-κB), we demonstrated that PVP-037.2/SE led to relative SEAP activity equivalent to that of R848 (Fig. 5E). To further assess the immunostimulatory profiles and synergistic effects of PVP-037.2/SE on primary immune cells, we stimulated adult mice BMDCs and BMDMs with increasing concentrations of each SE, PVP-037.2 and PVP-037.2/SE for 24 hours. We focused on TNF as a surrogate for the capacity to induce broad innate response. PVP-037.2/SE synergistically induced concentration-dependent TNF production in BMDCs (Fig. 5F) and BMDMs (Fig. 5G) while conversely reducing cytotoxicity of the emulsion alone (Fig. 5, H and I), respectively.

On the basis of these in vitro observations, we next evaluated the ability of PVP-037.2/SE to enhance anti-rHA Abs in vivo. To this end, using WT adult mice, we first determined 10 nmol of PVP-037.2 to be a minimally effective adjuvant dose for rHA (1/10th dose as compared to Figs. 3 and 4), with Ab titers for rHA-specific total IgG and IgG2c measured 42 days after immunization (Fig. 5J). Addition of 10 nmol of PVP-037.2/SE resulted in a 10-fold enhancement in both total IgG and IgG2c class switched Ab response (Fig. 5J), significantly enhancing the humoral response as compared to the rHA, rHA+ PVP-037.2 or rHA + SE (dotted line) groups.

DISCUSSION

Herein, we report the use of a human in vitro screen to identify an imidazopyrimidine TLR7/8A pharmacophore with innate immune enhancing activity in vitro and adjuvanticity in vivo. While TLR7/8As have considerable potential in the preclinical and clinical setting, their use can be limited by reactogenicity (*37*, *38*). Accordingly, advanced TLR7/8A formulations which promote targeted delivery and avert systemic inflammation, but still activate innate and adaptive immunity, are of substantial interest (*6*, *17*). Formulating small-molecule adjuvants offers significant advantages such as targeted activation of antigen presenting cells (APCs), increased stability of small molecules for longer duration, potential antigen-sparing effects, improved reactogenicity profiles, long-term safety, and efficacy (*39*). Hence, we focused on a formulation incorporating PVP-037.2 with O/W emulsion which significantly modified and enhanced the immune profile of the molecule.

In our present study, we used a phenotypic in vitro discovery approach using primary human PBMCs to identify an IMP pharmacophore, that when incorporated into an O/W emulsion, is a synergistically stable formulation in vitro with efficacy in vivo. Our study features several strengths, including (i) use of in vitro

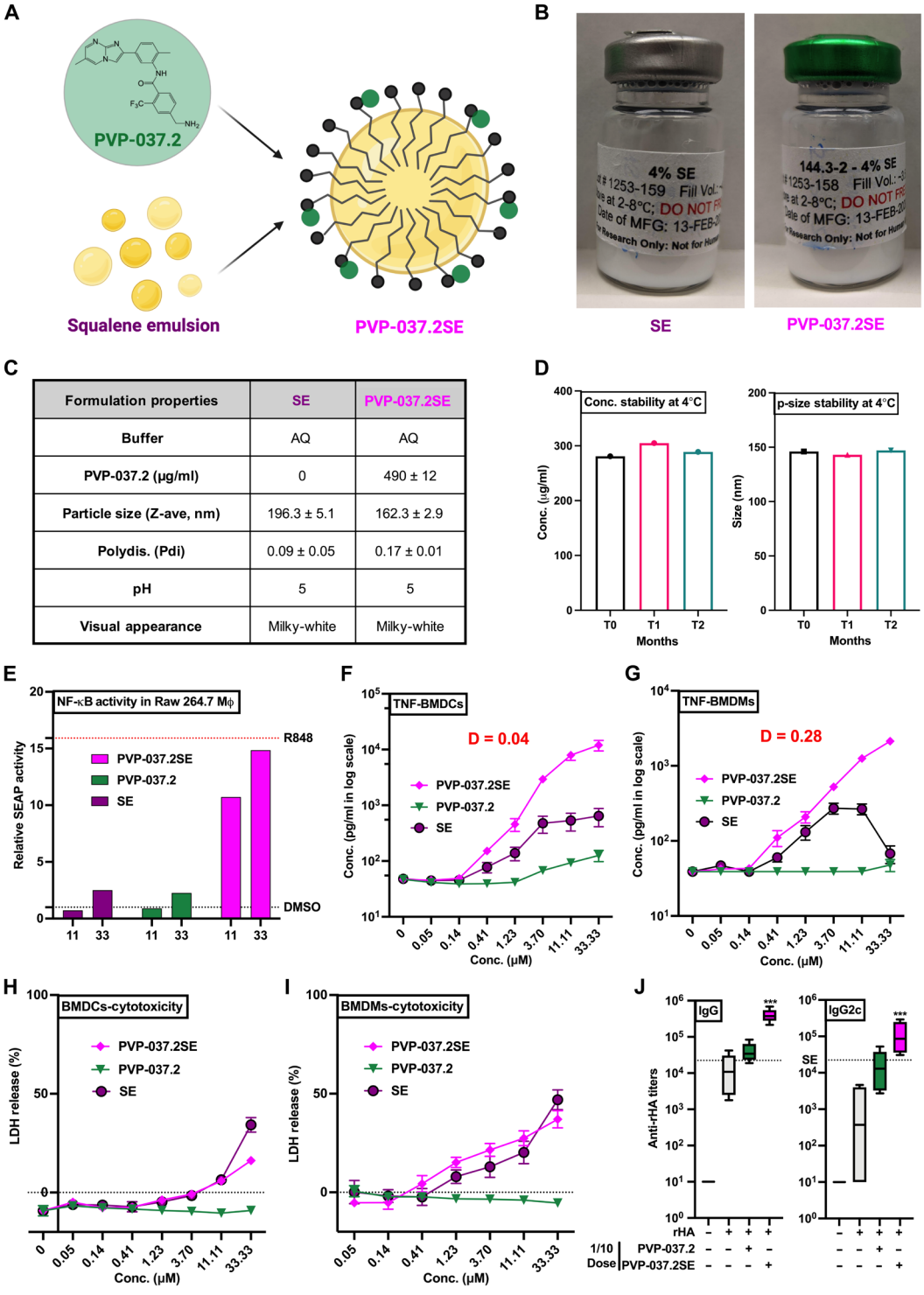

Formulation properties	SE	PVP-037.2SE
Buffer	AQ	AQ
PVP-037.2 (µg/ml)	0	490 ± 12
Particle size (Z-ave, nm)	196.3 ± 5.1	162.3 ± 2.9
Polydis. (Pdi)	0.09 ± 0.05	0.17 ± 0.01
pH	5	5
Visual appearance	Milky-white	Milky-white

Fig. 5. PVP-037.2 acts in synergy with a squalene-based oil in water formulation to enhance cytokine induction in vitro and vaccine immunogenicity in vivo. (**A**) Graphical representation depicting incorporation of PVP-037.2 in a squalene-based O/W emulsion. (**B**) Representative pictures of formulation vials, (**C**) formulation properties, and (**D**) concentration, particle-size stability, of compositions manufactured for PVP-037.2/SE formulation and the vehicle (SE). (**E**) RAW-Blue cells [murine RAW264.7 macrophage cell line expressing secreted embryonic alkaline phosphatase (SEAP) reporter construct inducible by NF-κB and AP-1] were stimulated with indicated concentrations of PVP-037.2, PVP-037.2/SE, SE, R848, or DMSO. After 20 to 24 hours, supernatants were harvested, and SEAP production was measured using QuantiBlue assay for assessing NF-κB activation. (**F**) BMDCs and (**G**) BMDMs were stimulated with indicated concentrations of PVP-037.2, PVP-037.2/SE, or SE for 20 to 24 hours and TNF production measured via ELISA ($n = 5$ samples). (**H** and **I**) In addition, cytotoxicity was measured in BMDCs and BMDMs using a lactate dehydrogenase (LDH) colorimetric assay kit, respectively. (**J**) WT mice (6 to 8 weeks old) were injected IM prime (day 0)/boost (day 28) with saline, rHA alone, and rHA admixed with the 10 nmol of PVP-037.2, PVP-037.2/SE, or SE. Ab titers for rHA-specific total IgG or IgG2c were measured by ELISA 42 days after immunization ($n = 5$ samples).

modeling using primary human PBMCs for a phenotypical drug discovery screen, (ii) discovery and development of a TLR7/8A adjuvant with broad immuno-stimulatory ability, (iii) creation of a well-defined O/W emulsion, and (iv) assessment of adjuvant combinations in vitro and in vivo.

Our study also has some limitations, including (i) mice may not accurately reflect in vivo effects in humans and future studies may benefit from porcine and/or nonhuman primate studies, (ii) while TLRs 7 and 8 appear to be important to PVP-037's action, we did not assess additional pathways that may contribute to activity such as the inflammasome (*40*), (iii) future functional studies including pathogen challenge could further assess adjuvant effects on vaccine efficacy, (iv) immunization studies were undertaken at relatively short timepoints, such that future studies are needed to assess the impact of PVP-037 on durability of immune responses, and although we focused on Ab responses as important correlates of protection against influenza and SARS-CoV-2 (*41*, *42*), (v) further studies should assess T cell responses, as cellular immunity provides an important layer of protection, along with toxicity studies on stable formulations. Last, although we screened molecules based on NF-κB and cytokine expression, additional endpoints such as costimulatory marker expressions (e.g., CD80, CD86, and OX40) are potentially valuable for future phenotypic HTS campaigns (*43*, *44*).

Historically, vaccine development has been largely limited to empirical approaches focused on infectious diseases and has targeted entire populations, potentially disregarding distinct immunity in vulnerable populations. Research has suggested that several factors can influence and thus alter the efficacy of vaccines, such as differences in immune status (healthy versus immunocompromised individuals) (*45*), sex, age (e.g., newborn/infant versus adult versus elder) (*46*, *47*) and geographical location (resulting in distinct genetic and epigenetic backgrounds) (*48*). Furthermore, effects of at least some combination adjuvants may vary with age (*49*). Thus, current approaches are ushering in an area of precision vaccinology aimed at tailoring immunization for vulnerable populations with distinct immunity, especially for pediatric use (*16*, *48*, *50*–*52*), where novel TLR7/8As have shown promise.

In summary, we report the discovery, characterization, and development of a TLR7/8A agonist IMP adjuvant formulation that may have utility for enhancing Th-polarizing immunity for a broad range of indications including as a stand-alone agent to treat viral infections or redirect immunity to treat allergy as well as an adjunctive adjuvant to enhance vaccine-induced immune responses and protection.

MATERIALS AND METHODS

Ethics statements

All experiments were conducted in accordance with relevant institutional and national guidelines, regulations and approvals. Experiments involving animals were approved by the Institutional Animal Care and Use Committees (IACUC) of Boston Children's Hospital and Harvard Medical School (protocol numbers 15-11-3011 and 16-02-3130). C57BL/6J, BALB/c, and *Tlr7*$^{-/-}$ mice were obtained from the Jackson Laboratory (Bar Harbor, ME), and housed in specific pathogen–free conditions in the animal research facilities at Boston Children's Hospital. Blood samples from adult volunteers were collected after written informed consent with approval from the Ethics Committee of Boston Children's Hospital, Boston, MA (protocol number X07-05-0223).

Overview of discovery approach

To identify small molecules that activate human leukocytes, screening of ~200,000 small molecules was first conducted via a THP1-Lucia based nuclear factor-kappa B (NF-κB)-dependent luminescence assay. As we postulated that cell culture lines such as THP-1 cells may not fully capture innate immune responses typical of primary human leukocytes, we next used a targeted HTS methodology in which ~10,000 compounds, made up from small-molecule library plates that had a relatively high number of hits/plate in the THP-1-Lucia screening campaign, were tested. This secondary PBMCs screening campaign was completed using primary human PBMCs from three different adult human donors in duplicate, therefore totaling ~60,000 individually screened treatment wells using a TNF focused Alpha-LISA Assay (PerkinElmer) (*53*).

Reporter cell lines and reagents

THP1-Lucia and RAW-Blue cell lines were obtained from Invivogen (San Diego, CA). THP1-Lucia cells, which are human monocytic cells derived from the blood of a pediatric patient with leukemia, contain an NF-κB–inducible luciferase (Luc) reporter construct. This allows NF-κB activation to be measured by quantifying the luminescence from the secreted Luc enzyme. RAW-Blue cells are derived from the murine RAW264.7 macrophages and contain an NF-κB/AP-1-inducible secreted embryonic alkaline phosphatase (SEAP) reporter gene. Both cell lines were cultured and used for assays according to the manufacturer's protocol. ODN 2088 and ODN 20958 were purchased from Miltenyi Biotec (MA, USA). Cytotoxicity detection kit (LDH) was purchased from Roche Diagnostics (CT, USA) and used as per manufacturer's protocol.

Chemical libraries

The compound libraries screened included known bioactive, academic and commercial libraries from various sources (e.g., ChemDiv, ChemBridge, and Asinex). All small molecules were dissolved in DMSO, typically at 10 mM, and libraries were stored at −20°C in desiccated storage containers. The small-molecule libraries were provided by and the high throughput screens described below were conducted at the ICCB-Longwood Screening Facility at Harvard Medical School. Further details describing each library used in this study appear in tables S1 and S2.

NF-κB–induced luminescence HTS assay

THP1-Lucia cells, between passages 15 and 18, and suspended in culture medium, were dispensed into 384-well black-walled clear-bottom plates (Corning 3712) at 30,000 cells in 30 μl per well using a Thermo Combi liquid dispenser. The following controls were included on each assay plate at the indicated final concentration in 0.3% DMSO: 50 μM R848, a TLR7/8A; 100 nM Phorbol myristate acetate (PMA); and 0.3% DMSO. Experimental compounds were added to duplicate assay plates using a custom pin transfer workstation, with 100 nl of compound in 100% DMSO added. For most small-molecule libraries, this resulted in a final compound concentration of 33 μM in 0.3% DMSO. Plates were then incubated for 24 hours at 37C with 5% CO_2 at 95% humidity. Following incubation, 10 μl of supernatant was removed from each well and transferred to a 384-well, white-walled, opaque microplate (Corning

3570) using an Agilent Vprep. 10 μl of recombinant Lucia protein (InvivoGen) diluted 1:2000 in THP1 culture media was added to empty well P24. Using a Combi liquid dispenser, 50 μl per well of Quanti-Luc substrate (InvivoGen) diluted 1:3 in sterile water was added to the assay plate. Immediately after substrate addition, the luminescence was quantitated by a PerkinElmer Envision plate reader.

AlphaLISA HTS assay

Human adult peripheral blood was collected according to approved protocols. PBMCs were isolated from blood using a Ficoll density gradient. PBMCs were stored at 5×10^7 cells per vial in 1 ml of RPMI containing 20% autologous plasma and 10% DMSO at −80°C until use. On day 1, PBMCs were thawed in 37°C water bath for 3 min and washed twice with Phosphate-buffered saline (PBS). Viability was assessed by trypan blue staining and cells were then resuspended to 6.67×10^5 viable cells/ml in DMEM with 10% autologous plasma. 30 μl of cells were dispensed per well in Corning 3712 black walled, clear bottom 384-cell culture plates, resulting in 20,000 cells per well). Controls and experimental compounds were added to cells as described above and plates were then incubated at 37°C, 5% CO_2 and 95% humidity for 18 hours. Following incubation, plates were centrifuged and 2 μl supernatant was aspirated and dispensed into Perkin Elmer Alpha plates using an Agilent Vprep. Following manufacturer instructions, the Perkin Elmer Human TNFα kits (cat# AL208F) were used to quantitate the TNF concentration in supernatants, with assay readout on the Perkin Elmer EnVision.

HTS hit calling method

Experimental compounds generating a robust Z score > 2 in both replicates for the THP-1 NF-κB induced Luc HTS assay and in ≥2 of the 3 human samples of PBMCs for the AlphaLISA HTS assay were considered potential hits. The statistical analyses used to identify potential hits in the THP-1 and TNF AlphaLISA assays are described in detail in the Supplementary Materials.

Collection of human blood, isolation, and in vitro assay of PBMCs

Peripheral blood was collected from healthy adult volunteers. Human experimentation guidelines of the U.S. Department of Health and Human Services and Boston, and Boston Children's Hospital were observed, following protocols approved by the local institutional review boards. Human blood was anti-coagulated with 20 units/ml pyrogen-free sodium heparin (American Pharmaceutical Partners Inc.; Schaumberg, IL). All blood products were kept at room temperature (RT) and processed within 4 hours from collection as previously described (*16*, *54*). PBMCs were isolated from blood using a Ficoll density gradient. PBMCs either used fresh or were stored at 5×10^7 cells per vial in 1 ml of RPMI containing 20% autologous plasma and 10% DMSO at −80°C until use. Stimulation plates were prepared by transferring 0.66 μl of DMSO-dissolved compounds (10 mM) to each well of a round bottom 96-well plate. PBMCs isolated from human adult donors were resuspended at a concentration of 10^5 cells / 200 μl of RPMI supplemented with 10% of platelet-poor plasma. The cell suspension (200 μl) was transferred to each well resulting in a final compound concentration (e.g., 33 μM). After ~18 hours of incubation (37°C, 5% CO_2), plates were centrifuged (500*g*, RT, 5 min), and supernatants were harvested for further analysis.

ELISAs and multiplex-Analyte assays

Supernatants derived from human PBMCs stimulations were assayed by ELISA for TNF (Thermo Fisher Scientific; Waltham, MA, USA). Cytokine and chemokine expression profiles (e.g., IFNγ, IL-9, IL-10, IL-12 (p70), IL-13, IL-1β, IL-23, IL-27, IL-28A, IL-33, IL-6, MIP-3α/CCL20, and TNF) in cell culture supernatants were measured using a customized Milliplex Human Th17 Magnetic Bead Panel according to the manufacturer's instructions (Millipore; Chicago, IL, USA). Assays were read and analyzed on the Luminex 100/200 System and xPOTENT software (Luminex; Austin, TX). A minimum threshold was set at the minimum detectable concentration for each individual assay, defined as three standard deviations above the mean background. Supernatants derived from murine bone marrow-derived dendritic cells (BMDCs), or macrophage stimulations were assayed by ELISA for TNF and/or IL-6 (Thermo Fisher Scientific).

Endotoxin measurement and human TLR-transfected HEK293 assay

All TLR7/8As in both in vitro and in vivo studies were verified to be free of endotoxin (< 1 EU/ml) by the Endosafe nexgen-MCS Limulus amoebocyte lysate assay per the manufacturer's instructions (Charles River Laboratories). HEK293 cells expressing human TLRs with an NF-κB–responsive secreted embryonic alkaline phosphatase (SEAP) reporter gene were obtained from Novus Biologicals (Littleton, CO) and InvivoGen (San Diego, CA), respectively. Cells were maintained in DMEM with 10% HI-FBS and selection antibiotics per the manufacturer's instructions. Cells were plated at 5×10^5 cells/96-well and stimulated with indicated agonist(s) for 24 hours. Supernatants were harvested and analyzed for NF-κB/SEAP activation using the QuantiBlue kit (InvivoGen). Values are expressed as fold change in optical density at 650 nm (OD_{650}) over vehicle-only treated samples.

Generation of human MoDCs, mouse splenocytes, macrophages, and dendritic cells

Monocytes were isolated from PBMC fractions by positive selection by magnetic microbeads according to the manufacturer's instructions (Miltenyi Biotec, Auburn, CA) using CD14 as a pan marker. Isolated monocytes were cultured in tissue culture dishes at 10^6 cells/ml in RPMI 1640 media containing fresh 10% autologous plasma, supplemented with recombinant human IL-4 (50 ng/ml) and recombinant human GM-CSF (100 ng/ml) (R&D Systems, Minneapolis, MN) with one additional supplement of fresh media and cytokines at day 3 of culture as previously described (*34*, *55*). After 6 days, immature MoDCs were harvested by gently pipetting the loosely adherent fraction, before being re-plated (10^5 cells per well) in 96-well U-bottom plates in the presence or absence of treatments and/or sterile PBS. Plates were then incubated for 18 to 24 hours at 37°C in a humidified incubator at 5% CO_2. After this stimulation supernatants were harvested and processed for further functional assays. To isolate murine splenocytes, spleens were mashed through a 70 μm cell strainer, and the resulting cell suspensions were washed with PBS and incubated with 2 mL of ACK lysis buffer (Gibco) for 2 min at RT to lyse erythrocytes. Splenocytes were washed again with PBS and plated in flat-bottom 96-well plates (2×10^6 cells per well) for stimulation for 48 hours, supernatants were harvested, and cytokine concentrations were measured by ELISA (*15*). Mouse

macrophages were derived from isolated bone marrow–derived progenitor cells via their propagation in M-CSF-containing medium. After 7 days in culture, with one additional supplement of fresh media and cytokines at day 3 of culture, contaminating nonadherent cells are eliminated by gently pipetting the loosely adherent fraction, adherent cells are harvested for assays, before being re-plated (10^5 cells/ well) in 96-well U-bottom plates in the presence or absence of treatments and/or sterile PBS. Adherent BMDMs are routinely >90% pure (*56*). Mouse bone-marrow derived dendritic cells (BMDCs) were generated as described previously (*57*).

Influenza antigens, vaccination and antibody quantification

For vaccination experiments, adult mice, typically 6 to 8 weeks of age (either C57BL/6J or BALB/c strains), and 56 weeks old (for aged BALB/c) were immunized intramuscularly (IM) in the right posterior thigh with 50 µl of vaccine dose containing 0.33 µg of each of the following recombinant influenza virus hemagglutinins (rHA): A/Michigan/45/2015 (H1N1), A/Hong Kong/4801/2014 (H3N2), and B/Brisbane/60/2008, derived from seasonal FluBlok vaccine (Protein Sciences Corp.). Mice were vaccinated with a prime-boost schedule (two injections) 4 weeks apart. Each vaccine dose was formulated with 10% (v/v) DMSO, except for the groups vaccinated with the IMP compounds since they were dissolved in DMSO and 5% (v/v) Tween-80. As indicated for specific experimental groups, each dose may have been also formulated with Aluminium hydroxide (100 µg) and/or PVP-037 or its analogs (each IMP at 100 nmol, final DMSO concentration 10%). Serum was collected 28 days after prime (preboost blood sample) and 14 days after boost for antibody detection. rHA-specific total IgG were quantified by ELISA. High binding flat bottom 96-well plates (Corning Life Sciences) were coated with rHA (1 µg/ml) in carbonate buffer pH 9.6, incubated overnight at 4°C and blocked with PBS + bovine serum albumin (BSA) 1% (Sigma-Aldrich) for 1 hour at RT. Then, sera from vaccinated mice were added with an initial dilution of 1:100 and 1:4 serial dilutions in PBS + BSA 1% and incubated for 2 hours at RT. Plates were then washed and incubated for 1 hour at RT with horseradish peroxidase (HRP)–conjugated anti-mouse IgG (Southern Biotech). At the end of the incubation plates were washed again and developed with tetramethylbenzidine (BD Biosciences) for 5 min, then stopped with 1 N H_2SO_4. The OD was read at 450 nm Versamax microplate reader with SoftMax Pro Version 5 (both from Molecular Devices) and endpoint titers were calculated using as cut-off three times the OD of the background.

SARS-CoV-2 WT spike and RBD expression/purification and serology

Full length SARS-CoV-2 Wuhan-Hu-1 spike glycoprotein (M1-Q1208, GenBank MN90894) and RBD constructs (amino acid residues R319-K529, GenBank MN975262.1), both with an HRV3C protease cleavage site, a TwinStrepTag and an 8XHisTag at C terminus were obtained from Barney S. Graham (NIH Vaccine Research Center) and Aaron G. Schmidt (Ragon Institute), respectively. These mammalian expression vectors were used to transfect Expi293F suspension cells (Thermo Fisher Scientific) using polyethylenimine (Polysciences). Cells were allowed to grow in 37°C, 8% CO_2 for an additional 5 days before harvesting for purification. Protein was purified in a PBS buffer (pH 7.4) from filtered supernatants by using either StrepTactin resin (IBA) or Cobalt-TALON resin (Takara). Affinity tags were cleaved off from eluted protein samples by HRV 3C protease, and tag removed proteins were further purified by size-exclusion chromatography using a Superose 6 10/300 column (Cytiva) for full length Spike and a Superdex 75 10/300 Increase column (Cytiva) for RBD domain in a PBS buffer (pH 7.4).

Mice were vaccinated as above. Spike protein–specific antibody titers were quantified in serum samples by ELISA by modification of a previously described protocol (*57*). Briefly, high-binding flat-bottom 96-well plates (Corning) were coated with spike protein (25 ng per well) and incubated overnight at 4°C. Plates were washed with 0.05% Tween 20/PBS and blocked with 1% BSA/PBS for 1 hour at RT. Serum samples were serially diluted fourfold from 1:100 up to 1:1.05 × 10^8 and then incubated for 2 hours at RT. Plates were washed three times and incubated for 1 hour at RT with HRP-conjugated anti-mouse IgG, IgG1, and IgG2a (SouthernBiotech). Plates were washed five times and developed with tetramethylbenzidine (BD OptEIA Substrate Solution, BD Biosciences) for 5 min and then stopped with 2 N H2SO4. Optical densities (ODs) were read at 450 nm with a SpectraMax iD3 microplate reader (Molecular Devices). To determine endpoint titers, five-parameter logistic asymmetric sigmoidal curves were generated (*15*, *45*, *58*, *59*). Endpoint titers were calculated as the dilution that emitted an OD matching a 3x background. An arbitrary value of 50 was assigned to the samples with OD values below the limit of detection for which it was not possible to interpolate the titer.

The hACE2-RBD inhibition assay used a modification of a previously published protocol (*60*). Briefly, high-binding flat-bottom 96- well plates (Corning) were coated with recombinant hACE2 (100 ng per well) (Sigma-Aldrich) in PBS, incubated overnight at 4°C, washed three times with 0.05% Tween 20 PBS, and blocked with 1% BSA PBS for 1 hour at RT. Serum samples were diluted 1:160, preincubated with 3 ng of WT RBD-Fc in 1% BSA PBS for 1 hour at RT, and then transferred to the hACE2-coated plate. RBD-Fc without preincubation with serum samples was added as a positive control, and 1% BSA PBS without serum preincubation was added as a negative control. Plates were then washed three times and incubated with HRP-conjugated anti-human IgG Fc (SouthernBiotech) for 1 hour at RT. Plates were washed five times and developed with tetramethylbenzidine (BD OptEIA Substrate Solution, BD Biosciences) for 5 min and then stopped with 2 N H_2SO_4. The OD was read at 450 nm with a SpectraMax iD3 microplate reader (Molecular Devices). Percentage inhibition of RBD binding to hACE2 was calculated as: Inhibition (%) = [1 − (Sample OD value − Negative Control OD value)/(Positive Control OD value − Negative Control OD value)] × 100.

IMPs: Synthesis and formulation

IMPs were synthesized following established procedures, as described in WO2019099564. A representative example is shown in "Preparation of example S1" in the Supplementary Materials, Other IMPs were prepared by similar methods to examples S1 and S2, from the corresponding aniline and either the acid chloride or carboxylic acid. For IMP formulations, squalene was obtained from Sigma. Phospholipids (DMPC, DPPG) were purchased from Lipoid or NOF. Ammonium phosphate monobasic, ammonium phosphate dibasic, and hydrochloric acid (HCl) were acquired from J.T. Baker. Poloxamer 188 and glycerol were obtained from Spectrum Chemical. PBS was supplied by Gibco. Acrodisc PES 0.8/0.2 µm syringe filters were acquired from Pall. G2 Slide-A-Lyzer dialysis cassettes (2,000 MWCO) were obtained from Thermo Fisher Scientific. Ethanol

was purchased from Fischer Scientific. PVP-037.2/SE O/W emulsion formulation of compound PVP-037.2 was prepared by adding 0.2 ml of squalene, 61 mg DMPC, 12 mg DPPG, 2 mg poloxamer 188, and 4 mg of compound PVP-037.2 (i.e., 0.5 ml solution of 8 mg/ml compound PVP-037.2 in ethanol and 0.2 v/v% HCl) to 4.5 ml of 25 mM ammonium phosphate buffer (pH 5.7) containing 24 mg/mL glycerol. The mixture was sonicated at 60–70°C for 4–6 hours, followed by dialyzing overnight in 25 mM ammonium phosphate buffer (pH 5.7) containing 24 mg/ml glycerol. Last, dialyzed formulation was filtered in a laminar flow hood, filled into a glass vial, and stored at 2–8°C. Blank emulsions were manufactured in a similar manner but without compound. Characterization of the emulsion formulations consisted of dynamic light scattering (following 50 - fold dilution in water) to measure particle diameter (Malvern Nano-S or -ZS), absorbance at 326 nm to measure compound concentration (Agilent Cary 100), and visual appearance. Formulation characteristics are listed in Fig. 5.

Statistical analyses and graphics

Statistical significance and graphical outputs were generated using GraphPad Prism version 8 for macOS (GraphPad Software; La Jolla, CA, USA) and Microsoft Excel (Microsoft Corporation; Redmond, WA). For non-HTS in vitro and in vivo experiments where values were normalized to control, column statistics were conducted using two-tailed Wilcoxon signed-rank test or one-sample *t*-test comparing to control. Group comparisons were performed by one-way analysis of variance (ANOVA) with Dunnett's multiple comparison post-test or two-way ANOVA comparing column and row effects. Results were considered significant at $P < 0.05$, and indicated as follows: $*P < 0.05$, $**P < 0.01$, $***P < 0.001$, $****P < 0.0001$. Synergy was evaluated using the Loewe definition of additivity, with $D > 1$ indicating antagonism, $D = 1$ additivity, and $D < 1$ synergy (*49*, *61*). To fit regression curves more closely to the data, higher concentrations were excluded from linear regressions when calculating D values if the cytokine concentrations plateaued or decreased. Graphics were created with BioRender.com.

Data management and availability

D.S. conducted Data Quality Control (QC) by screening all submitted figures against the raw data provided. D.J.D. carried out Quality assurance (QA) by screening of a ~10% random sample data (2 randomly selected figures/tables, from ~20 total). All data needed to evaluate the conclusions in this article are present in the paper and/or included in the supplementary materials.

Supplementary Materials

This PDF file includes:

Supplementary Text
Figs. S1 to S10
Tables S1 to S3
Legend for data S1

Other Supplementary Material for this manuscript includes the following:

Data S1

REFERENCES AND NOTES

1. D. Soni, S. D. van Haren, O. T. Idoko, J. T. Evans, J. Diray-Arce, D. J. Dowling, O. Levy, Towards precision vaccines: Lessons from the second international precision vaccines conference. *Front. Immunol.* **11**, 590373 (2020).
2. L. Shaffer, Using vaccines to harness the immune system and fight drugs of abuse. *Proc. Natl. Acad. Sci. U S A* **118**, e2121094118 (2021).
3. O. J. Finn, The dawn of vaccines for cancer prevention. *Nat. Rev. Immunol.* **18**, 183–194 (2018).
4. M. D. Raleigh, M. Laudenbach, F. Baruffaldi, S. J. Peterson, M. J. Roslawski, A. K. Birnbaum, F. I. Carroll, S. P. Runyon, S. Winston, P. R. Pentel, M. Pravetoni, Opioid dose- and route-dependent efficacy of oxycodone and heroin vaccines in rats. *J. Pharmacol. Exp. Ther.* **365**, 346–353 (2018).
5. B. Crouse, S. M. Miller, P. Muelken, L. Hicks, J. R. Vigliaturo, C. L. Marker, A. G. P. Guedes, P. R. Pentel, J. T. Evans, M. G. LeSage, M. Pravetoni, A TLR7/8 agonist increases efficacy of anti-fentanyl vaccines in rodent and porcine models. *NPJ Vaccines* **8**, 107 (2023).
6. E. Nanishi, D. J. Dowling, O. Levy, Toward precision adjuvants: optimizing science and safety. *Curr. Opin. Pediatr.* **32**, 125–138 (2020).
7. D. Soni, S. Bobbala, S. Li, E. A. Scott, D. J. Dowling, The sixth revolution in pediatric vaccinology: immunoengineering and delivery systems. *Pediatr. Res.* **89**, 1364–1372 (2021).
8. S. G. Reed, M. Tomai, M. J. Gale Jr., New horizons in adjuvants for vaccine development. *Curr. Opin. Immunol.* **65**, 97–101 (2020).
9. B. Pulendran, P. S. Arunachalam, D. T. O'Hagan, Emerging concepts in the science of vaccine adjuvants. *Nat. Rev. Drug Discov.*, 1–22 (2021).
10. S. Barman, D. Soni, B. Brook, E. Nanishi, D. J. Dowling, Precision vaccine development: Cues from natural immunity. *Front. Immunol.* **12**, 662218 (2021).
11. B. Pulendran, P. S. Arunachalam, D. T. O'Hagan, Emerging concepts in the science of vaccine adjuvants. *Nat. Rev. Drug Discov.* **20**, 454–475 (2021).
12. D. T. O'Hagan, R. N. Lodaya, G. Lofano, The continued advance of vaccine adjuvants–'we can work it out'. *Semin. Immunol.* **50**, 101426 (2020).
13. S. A. Plotkin, W. A. Orenstein, P. A. Offit, *Vaccines* (Elsevier Saunders, ed. 6, 2012).
14. R. Rappuoli, A. Aderem, A 2020 vision for vaccines against HIV, tuberculosis and malaria. *Nature* **473**, 463–469 (2011).
15. E. Nanishi, F. Borriello, T. R. O'Meara, M. E. McGrath, Y. Saito, R. E. Haupt, H. S. Seo, S. D. van Haren, C. B. Cavazzoni, B. Brook, S. Barman, J. Chen, J. Diray-Arce, S. Doss-Gollin, M. de Leon, A. Prevost-Reilly, K. Chew, M. Menon, K. Song, A. Z. Xu, T. M. Caradonna, J. Feldman, B. M. Hauser, A. G. Schmidt, A. C. Sherman, L. R. Baden, R. K. Ernst, C. Dillen, S. M. Weston, R. M. Johnson, H. L. Hammond, R. Mayer, A. Burke, M. E. Bottazzi, P. J. Hotez, U. Strych, A. Chang, J. Yu, P. T. Sage, D. H. Barouch, S. Dhe-Paganon, I. Zanoni, A. Ozonoff, M. B. Frieman, O. Levy, D. J. Dowling, An aluminum hydroxide:CpG adjuvant enhances protection elicited by a SARS-CoV-2 receptor binding domain vaccine in aged mice. *Sci. Transl. Med.* **14**, eabj5305 (2022).
16. D. J. Dowling, S. D. van Haren, A. Scheid, I. Bergelson, D. Kim, C. J. Mancuso, W. Foppen, A. Ozonoff, L. Fresh, T. B. Theriot, A. A. Lackner, R. N. Fichorova, D. Smirnov, J. P. Vasilakos, J. M. Beaurline, M. A. Tomai, C. C. Midkiff, X. Alvarez, J. L. Blanchard, M. H. Gilbert, P. P. Aye, O. Levy, TLR7/8 adjuvant overcomes newborn hyporesponsiveness to pneumococcal conjugate vaccine at birth. *JCI Insight* **2**, e91020 (2017).
17. D. J. Dowling, Recent advances in the discovery and delivery of TLR7/8 agonists as vaccine adjuvants. *Immunohorizons* **2**, 185–197 (2018).
18. S. G. Reed, M. T. Orr, C. B. Fox, Key roles of adjuvants in modern vaccines. *Nat. Med.* **19**, 1597–1608 (2013).
19. G. Hu, Y. Su, B. H. Kang, Z. Fan, T. Dong, D. R. Brown, J. Cheah, K. D. Wittrup, J. Chen, High-throughput phenotypic screen and transcriptional analysis identify new compounds and targets for macrophage reprogramming. *Nat. Commun.* **12**, 773 (2021).
20. S. H. Spangenberg, R. B. Zavareh, L. L. Lairson, Protocol for high-throughput compound screening using flow cytometry in THP-1 cells. *STAR Protoc.* **2**, 100400 (2021).
21. P. T. Wong, P. R. Leroueil, D. M. Smith, S. Ciotti, A. U. Bielinska, K. W. Janczak, C. H. Mullen, J. V. Groom, E. M. Taylor, C. Passmore, P. E. Makidon, J. J. O'Konek, A. Myc, T. Hamouda, J. R. Baker, Formulation, high throughput *in vitro* screening and *in vivo* functional characterization of nanoemulsion-based intranasal vaccine adjuvants. *PLOS ONE* **10**, e0126120 (2015).
22. A. Dunne, M. Jowett, S. Rees, in *High Throughput Screening: Methods and Protocols*, *Second Edition*, W. P. Janzen, P. Bernasconi, Eds. (Humana Press, 2009), pp. 239–257.
23. S. Bournazos, J. V. Ravetch, Fcγ receptor function and the design of vaccination strategies. *Immunity* **47**, 224–233 (2017).
24. B. M. Gunn, G. Alter, Modulating antibody functionality in infectious disease and vaccination. *Trends Mol. Med.* **22**, 969–982 (2016).
25. J. T. Evans, L. S. Bess, S. C. Mwakwari, M. T. Livesay, Y. Li, V. Cybulski, D. A. Johnson, H. G. Bazin, Synthetic Toll-like receptors 7 and 8 agonists: Structure-activity relationship in the oxoadenine series. *ACS omega* **4**, 15665–15677 (2019).
26. G. Galli, D. Medini, E. Borgogni, L. Zedda, M. Bardelli, C. Malzone, S. Nuti, S. Tavarini, C. Sammicheli, A. K. Hilbert, V. Brauer, A. Banzhoff, R. Rappuoli, G. del Giudice, F. Castellino, Adjuvanted H5N1 vaccine induces early CD4+ T cell response that predicts long-term persistence of protective antibody levels. *Proc. Natl. Acad. Sci. U.S.A.* **106**, 3877–3882 (2009).

27. A. L. Wilkins, D. Kazmin, G. Napolitani, E. A. Clutterbuck, B. Pulendran, C. A. Siegrist, A. J. Pollard, AS03- and MF59-adjuvanted influenza vaccines in children. *Front. Immunol.* **8**, 1760 (2017).
28. N. Garcon, D. W. Vaughn, A. M. Didierlaurent, Development and evaluation of AS03, an Adjuvant System containing α-tocopherol and squalene in an oil-in-water emulsion. *Expert Rev. Vaccines* **11**, 349–366 (2012).
29. J. K. Tom, T. J. Albin, S. Manna, B. A. Moser, R. C. Steinhardt, A. P. Esser-Kahn, Applications of immunomodulatory immune synergies to adjuvant discovery and vaccine development. *Trends Biotechnol.* **37**, 373–388 (2019).
30. T. K. Ghosh, D. J. Mickelson, J. C. Solberg, K. E. Lipson, J. R. Inglefield, S. S. Alkan, TLR-TLR cross talk in human PBMC resulting in synergistic and antagonistic regulation of type-1 and 2 interferons, IL-12 and TNF-alpha. *Int. Immunopharmacol.* **7**, 1111–1121 (2007).
31. P. Ganesan, D. Narayanasami, Lipid nanoparticles: Different preparation techniques, characterization, hurdles, and strategies for the production of solid lipid nanoparticles and nanostructured lipid carriers for oral drug delivery. *Sustain. Chem. Pharm.* **6**, 37–56 (2017).
32. V. Iyer, C. Cayatte, B. Guzman, K. Schneider-Ohrum, R. Matuszak, A. Snell, G. M. Rajani, M. P. McCarthy, B. Muralidhara, Impact of formulation and particle size on stability and immunogenicity of oil-in-water emulsion adjuvants. *Hum. Vaccin. Immunother.* **11**, 1853–1864 (2015).
33. G. Napolitani, A. Rinaldi, F. Bertoni, F. Sallusto, A. Lanzavecchia, Selected Toll-like receptor agonist combinations synergistically trigger a T helper type 1-polarizing program in dendritic cells. *Nat. Immunol.* **6**, 769–776 (2005).
34. D. J. Dowling, E. A. Scott, A. Scheid, I. Bergelson, S. Joshi, C. Pietrasanta, S. Brightman, G. Sanchez-Schmitz, S. D. van Haren, J. Ninković, D. Kats, C. Guiducci, A. de Titta, D. K. Bonner, S. Hirosue, M. A. Swartz, J. A. Hubbell, O. Levy, Toll-like receptor 8 agonist nanoparticles mimic immunomodulating effects of the live BCG vaccine and enhance neonatal innate and adaptive immune responses. *J. Allergy Clin. Immunol.* **140**, 1339–1350 (2017).
35. L. Rossmann, K. Bagola, T. Stephen, A.-L. Gerards, B. Walber, A. Ullrich, S. Schülke, C. Kamp, I. Spreitzer, M. Hasan, B. David-Watine, S. L. Shorte, M. Bastian, G. van Zandbergen, Distinct single-component adjuvants steer human DC-mediated T-cell polarization via Toll-like receptor signaling toward a potent antiviral immune response. *Proc. Natl. Acad. Sci. U.S.A.* **118**, e2103651118 (2021).
36. R. J. Darling, S. Senapati, S. M. Kelly, M. L. Kohut, B. Narasimhan, M. J. Wannemuehler, STING pathway stimulation results in a differentially activated innate immune phenotype associated with low nitric oxide and enhanced antibody titers in young and aged mice. *Vaccine* **37**, 2721–2730 (2019).
37. S. L. Spruance, S. K. Tyring, M. H. Smith, T. C. Meng, Application of a topical immune response modifier, resiquimod gel, to modify the recurrence rate of recurrent genital herpes: a pilot study. *J Infect Dis* **184**, 196–200 (2001).
38. R. M. Szeimies, J. Bichel, J. P. Ortonne, E. Stockfleth, J. Lee, T. C. Meng, A phase II dose-ranging study of topical resiquimod to treat actinic keratosis. *Br. J. Dermatol.* **159**, 205–210 (2008).
39. Q. Yin, W. Luo, V. Mallajosyula, Y. Bo, J. Guo, J. Xie, M. Sun, R. Verma, C. Li, C. M. Constantz, L. E. Wagar, J. Li, E. Sola, N. Gupta, C. Wang, O. Kask, X. Chen, X. Yuan, N. C. Wu, J. Rao, Y. H. Chien, J. Cheng, B. Pulendran, M. M. Davis, A TLR7-nanoparticle adjuvant promotes a broad immune response against heterologous strains of influenza and SARS-CoV-2. *Nat. Mater.* **22**, 380–390 (2023).
40. V. J. Philbin, D. J. Dowling, L. C. Gallington, G. Cortés, Z. Tan, E. E. Suter, K. W. Chi, A. Shuckett, L. Stoler-Barak, M. Tomai, R. L. Miller, K. Mansfield, O. Levy, Imidazoquinoline Toll-like receptor 8 agonists activate human newborn monocytes and dendritic cells through adenosine-refractory and caspase-1-dependent pathways. *J. Allergy Clin. Immunol.* **130**, 195–204.e9 (2012).
41. F. Krammer, The human antibody response to influenza A virus infection and vaccination. *Nat. Rev. Immunol.* **19**, 383–397 (2019).
42. K. S. Corbett, M. C. Nason, B. Flach, M. Gagne, S. O'Connel, T. S. Johnston, S. N. Shah, V. V. Edara, K. Floyd, L. Lai, C. McDanal, J. R. Francica, B. Flynn, K. Wu, A. Choi, M. Koch, O. M. Abiona, A. P. Werner, J. I. Moliva, S. F. Andrew, M. M. Donaldson, J. Fintzi, D. R. Flebbe, E. Lamb, A. T. Noe, S. T. Nurmukhambetova, S. J. Provost, A. Cook, A. Dodson, A. Faudree, J. Greenhouse, S. Kar, L. Pessaint, M. Porto, K. Steingrebe, D. Valentin, S. Zouantcha, K. W. Bock, M. Minai, B. M. Nagata, R. van de Wetering, S. Boyoglu-Barnum, K. Leung, W. Shi, E. S. Yang, Y. Zhang, J.-P. M. Todd, L. Wang, G. S. Alvarado, H. Andersen, K. E. Foulds, D. K. Edwards, J. R. Mascola, I. N. Moore, M. G. Lewis, A. Carfi, D. Montefiori, M. S. Suthar, A. McDermott, M. Roederer, N. J. Sullivan, D. C. Douek, B. S. Graham, R. A. Seder, Immune correlates of protection by mRNA-1273 vaccine against SARS-CoV-2 in nonhuman primates. *Science* **373**, eabj0299 (2021).
43. K. Chew, B. Lee, A. Ozonoff, J. A. Smith, O. Levy, D. J. Dowling, S. van Haren, A protocol for high-throughput screening for immunomodulatory compounds using human primary cells. *STAR protoc.* **4**, 102405 (2023).
44. K. Chew, B. Lee, S. D. van Haren, E. Nanishi, T. O'Meara, J. B. Splaine, M. DeLeon, D. Soni, H.-S. Seo, S. Dhe-Paganon, A. Ozonoff, J. A. Smith, O. Levy, D. J. Dowling, Adjuvant discovery via a high throughput screen using human primary mononuclear cells. bioRxiv 2022.06.17.496630 [**Preprint**]. 18 June 2022. https://doi.org/10.1101/2022.06.17.496630.
45. T. R. O'Meara, E. Nanishi, M. E. McGrath, S. Barman, D. Dong, C. Dillen, M. Menon, H. S. Seo, S. Dhe-Paganon, R. K. Ernst, O. Levy, M. B. Frieman, D. J. Dowling, Reduced SARS-CoV-2 mRNA vaccine immunogenicity and protection in mice with diet-induced obesity and insulin resistance. *J. Allergy Clin. Immunol.* **152**, 1107–1120.e6 (2023).
46. D. J. Dowling, O. Levy, A precision adjuvant approach to enhance severe acute respiratory syndrome coronavirus 2 (SARS-CoV-2) vaccines optimized for immunologically distinct vulnerable populations. *Clin. Infect. Dis.* **75**, S30–s36 (2022).
47. E. Nanishi, A. Angelidou, C. Rotman, D. J. Dowling, O. Levy, A. Ozonoff, Precision vaccine adjuvants for older adults: A scoping review. *Clin. Infect. Dis.* **75**, S72–S80 (2022).
48. B. Lee, E. Nanishi, O. Levy, D. J. Dowling, Precision vaccinology approaches for the development of adjuvanted vaccines targeted to distinct vulnerable populations. *Pharmaceutics* **15**, (2023).
49. S. D. van Haren, D. J. Dowling, W. Foppen, D. Christensen, P. Andersen, S. G. Reed, R. M. Hershberg, L. R. Baden, O. Levy, Age-specific adjuvant synergy: Dual TLR7/8 and mincle activation of human newborn dendritic cells enables Th1 polarization. *J. Immunol.* **197**, 4413–4424 (2016).
50. D. J. Dowling, O. Levy, Ontogeny of early life immunity. *Trends Immunol.* **35**, 299–310 (2014).
51. D. J. Dowling, S. Barman, A. J. Smith, F. Borriello, D. Chaney, S. E. Brightman, G. Melhem, B. Brook, M. Menon, D. Soni, S. Schüller, K. Siram, E. Nanishi, H. G. Bazin, D. J. Burkhart, O. Levy, J. T. Evans, Development of a TLR7/8 agonist adjuvant formulation to overcome early life hyporesponsiveness to DTaP vaccination. *Sci. Rep.* **12**, 16860 (2022).
52. S. Barman, F. Borriello, B. Brook, C. Pietrasanta, M. de Leon, C. Sweitzer, M. Menon, S. D. van Haren, D. Soni, Y. Saito, E. Nanishi, S. Yi, S. Bobbala, O. Levy, E. A. Scott, D. J. Dowling, Shaping neonatal immunization by tuning the delivery of synergistic adjuvants via nanocarriers. *ACS Chem. Biol.* **17**, 2559–2571 (2022).
53. A. Schildberger, E. Rossmanith, T. Eichhorn, K. Strassl, V. Weber, Monocytes, peripheral blood mononuclear cells, and THP-1 cells exhibit different cytokine expression patterns following stimulation with lipopolysaccharide. *Mediators Inflamm.* **2013**, 697972 (2013).
54. D. J. Dowling, Z. Tan, Z. M. Prokopowicz, C. D. Palmer, M. A. H. Matthews, G. N. Dietsch, R. M. Hershberg, O. Levy, The ultra-potent and selective TLR8 agonist VTX-294 activates human newborn and adult leukocytes. *PLOS ONE* **8**, e58164 (2013).
55. L. Ganapathi, S. van Haren, D. J. Dowling, I. Bergelson, N. M. Shukla, S. S. Malladi, R. Balakrishna, H. Tanji, U. Ohto, T. Shimizu, S. A. David, O. Levy, The imidazoquinoline toll-like receptor-7/8 agonist hybrid-2 potently induces cytokine production by human newborn and adult leukocytes. *PLOS ONE* **10**, e0134640 (2015).
56. X. Zhang, R. Goncalves, D. M. Mosser, The isolation and characterization of murine macrophages. *Cur. Protoc. Immunol.* **Chapter 14**, Unit 14.11 (2008).
57. F. Borriello, C. Pietrasanta, J. C. Y. Lai, L. M. Walsh, P. Sharma, D. N. O'Driscoll, J. Ramirez, S. Brightman, L. Pugni, F. Mosca, D. J. Burkhart, D. J. Dowling, O. Levy, Identification and characterization of stimulator of interferon genes as a robust adjuvant target for early life immunization. *Front. Immunol.* **8**, 1772 (2017).
58. E. Nanishi, F. Borriello, H. S. Seo, T. R. O'Meara, M. E. McGrath, Y. Saito, J. Chen, J. Diray-Arce, K. Song, A. Z. Xu, S. Barman, M. Menon, D. Dong, T. M. Caradonna, J. Feldman, B. M. Hauser, A. G. Schmidt, L. R. Baden, R. K. Ernst, C. Dillen, J. Yu, A. Chang, L. Hilgers, P. P. Platenburg, S. Dhe-Paganon, D. H. Barouch, A. Ozonoff, I. Zanoni, M. B. Frieman, D. J. Dowling, O. Levy, Carbohydrate fatty acid monosulphate: Oil-in-water adjuvant enhances SARS-CoV-2 RBD nanoparticle-induced immunogenicity and protection in mice. *NPJ Vaccines* **8**, 18 (2023).
59. E. Nanishi, M. E. McGrath, T. R. O'Meara, S. Barman, J. Yu, H. Wan, C. A. Dillen, M. Menon, H. S. Seo, K. Song, A. Z. Xu, L. Sebastian, B. Brook, A. N. Bosco, F. Borriello, R. K. Ernst, D. H. Barouch, S. Dhe-Paganon, O. Levy, M. B. Frieman, D. J. Dowling, mRNA booster vaccination protects aged mice against the SARS-CoV-2 Omicron variant. *Commun. Biol.* **5**, 790 (2022).
60. C. W. Tan, W. N. Chia, X. Qin, P. Liu, M. I. C. Chen, C. Tiu, Z. Hu, V. C. W. Chen, B. E. Young, W. R. Sia, Y. J. Tan, R. Foo, Y. Yi, D. C. Lye, D. E. Anderson, L. F. Wang, A SARS-CoV-2 surrogate virus neutralization test based on antibody-mediated blockage of ACE2-spike protein-protein interaction. *Nat. Biotechnol.* **38**, 1073–1078 (2020).
61. M. C. Berenbaum, Correlations between methods for measurement of synergy. *J Infect Dis* **142**, 476–478 (1980).

Acknowledgments: We thank B. S. Graham (NIH Vaccine Research Center) for providing the plasmid for prefusion stabilized SARS-CoV-2 spike trimer. In addition, we would like to thank H.-S. Seo and S. Dhe-Paganon (at Department of Cancer Biology, Dana-Farber Cancer Institute, Boston, MA) for providing purified SARS-CoV-2 spike protein. Members of the BCH *Precision Vaccines Program* (PVP) are acknowledged for helpful discussions. We thank K. Churchwell, W. Chung, G. Fleisher, and N. Williams, as well as A. Cervini for support of the PVP. D.J.D. would like to thank S. McHugh, G. Boyer, L. Conetta, and the staff of Lucy's Daycare, the staff the YMCA of Greater Boston, Bridging Independent Living Together (BILT) Inc., and the Boston

Public Schools for childcare and educational support during the COVID-19 pandemic. Mass spectrometry work by M.C. was supported in part via NIH equipment grant 1 S10OD030332-01. **Funding:** The current study was supported in part by U.S. National Institutes of Health (NIH)/National Institutes of Allergy and Infectious Diseases (NIAID) awards, including Adjuvant Discovery (HHSN272201400052C) and Development (HHSN272201800047C) Program contracts (to O.L.) and an Adjuvant Discovery Program contract (75N93019C00044) to O.L. and D.J.D.; as well as NIH grant (1R21AI137932-01A1) to D.J.D. The *Precision Vaccines Program* is supported in part by the BCH Department of Pediatrics and the Chief Scientific Office. **Author contributions:** D.S. and D.J.D. wrote the first manuscript draft. D.J.D., S.E.B., W.K.C., J.A.S., S.D.v.H., M.A.P., and O.L. conceived, designed, performed, and analyzed HTS experiments. D.J.D., D.A.S., and F.F. designed and synthesized new compounds. D.S., F.B., S.E.B., and D.J.D. conceived, designed, performed, and analyzed the in vitro and in vivo experiments to optimize adjuvanted formulation. D.S., M.D., G.M., J.C.R., S.B., A.K., K.W., and E.N. performed mouse serological assays, splenocyte restimulation, and human in vitro experiments and assisted with analysis. D.S., D.J.D., and M.C. oversaw PK studies. C.B.F., T.P., Y.Q., R.K., M.M.R., and J.A.H. helped conceive and generate adjuvanted formulation. A.O. provided study design feedback and contributed to the statistical analysis. O.L. and D.J.D. conceived the project, secured funding, provided supervision, and oversaw final manuscript preparation. All authors reviewed and approved the version for publication. **Competing interests:** F.B., D.A.S., S.E.B., F.F., O.L., and D.J.D. are named inventors on patent for PVP-037 and related analogs, filed by Children's Medical Center Corp and Dana Farber Cancer Institute Inc. (USPTO no. patent US11673891B2), active from 13 June 2023. In addition, D.S., D.A.S., O.L., and D.J.D. have filed a provisional patent application for formulations and related analogs of PVP-037.2 (USPTO no. 63/437,902). F.B. has signed consulting agreements with Merck Sharp & Dohme Corp. (a subsidiary of Merck & Co. Inc.), Sana Biotechnology Inc., and F. Hoffmann–La Roche Ltd. O.L. served as a paid consultant to Moody's Analytics, GSK, and Hillevax. C.B.F. is on the scientific advisory board of MaxVax. D.J.D. is on the scientific advisory board of EdJen BioTech and serves as a consultant with Merck Research Laboratories/Merck Sharp & Dohme Corp. (a subsidiary of Merck & Co. Inc.). O.L. and D.J.D. are cofounders of Ovax Inc. All other authors declare they have no competing interests. **Data and materials availability:** Contingent on scientific review and a fully executed material transfer agreement with Boston Children's Hospital Technology & Innovation Development Office, PVP-037 (analogs and formulations) and/or access to the broader "PVP Adjuvant Portfolio," will be provided by the PVP team upon request as submitted to D.J.D. or O.L. All data needed to evaluate the conclusions in the paper are present in the paper and/or the Supplementary Materials.

Submitted 12 February 2023
Accepted 29 May 2024
Published 3 July 2024
10.1126/sciadv.adg3747